JOURNAL OF NATURAL PRODUCTS

Article

Cite This: J. Nat. Prod. 2018, 81, 811−817

pubs.acs.org/jnp

Drimane Sesquiterpenoids Noncompetitively Inhibit Human α4β2 Nicotinic Acetylcholine Receptors with Higher Potency Compared to Human α3β4 and α7 Subtypes

Hugo R. Arias,[†] Dominik Feuerbach,[‡] Bernd Schmidt,[§] Matthias Heydenreich,[§] Cristian Paz,*[,⊥] and Marcelo O. Ortells[∥]

[†]Department of Basic Sciences, California Northstate University College of Medicine, Elkgrove, California 95757, United States

[‡]Novartis Institutes for Biomedical Research, Basel CH-4057, Switzerland

[§]Department of Chemistry, University of Potsdam, D-14469 Potsdam, Germany

[⊥]Departamento de Química y Recursos Naturales, Universidad de La Frontera, Francisco Salazar 01145, Temuco, Chile

[∥]Facultad de Medicina, Universidad de Morón and CONICET, Morón 1708, Argentina

Supporting Information

ABSTRACT: The drimane sesquiterpenoids drimenin, cinnamolide, dendocarbin A, and polygodial were purified from the Canelo tree (*Drimys winteri*) and chemically characterized by spectroscopic methods. The pharmacological activity of these natural compounds were determined on hα4β2, hα3β4, and hα7 nicotinic acetylcholine receptors (AChRs) by Ca^{2+} influx measurements. The results established that drimane sesquiterpenoids inhibit AChRs with the following selectivity: hα4β2 > hα3β4 > hα7. In the case of hα4β2 AChRs, the following potency rank order was determined (IC_{50}'s in μM): drimenin (0.97 ± 0.35) > cinnamolide (1.57 ± 0.36) > polygodial (62.5 ± 19.9) ≫ dendocarbin A (no activity). To determine putative structural features underlying the differences in inhibitory potency at hα4β2 AChRs, additional structure−activity relationship and molecular docking experiments were performed. The Ca^{2+} influx and structural results supported a noncompetitive mechanism of inhibition, where drimenin interacted with luminal and nonluminal (TMD-β2 intrasubunit) sites. The structure−activity relationship results, i.e., the lower the ligand polarity, the higher the inhibitory potency, supported the nonluminal interaction. Ligand binding to both sites might inhibit the hα4β2 AChR by a cooperative mechanism, as shown experimentally (n_H > 1). Drimenin could be used as a molecular scaffold for the development of more potent inhibitors with higher selectivity for the hα4β2 AChR.

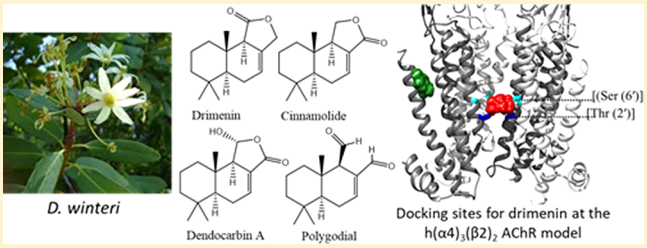

Nicotinic acetylcholine receptors (AChRs) are members of the Cys-loop ion channel superfamily, comprising $GABA_A$, glycine, and serotonin type 3 receptors.[1] Specific AChR subtypes are expressed in different brain areas, modulating many physiologically vital functions, including cognition, learning, memory, arousal, pain signaling, reward, neuroprotection, ganglia homeostasis, and regulation of immune responses.[2,3] Since the malfunctioning or imbalance of AChRs may evolve in important neurological diseases, including epilepsy, Alzheimer's disease, nicotine and drug addictions, chronic pain, depression, and anxiety,[2−5] the search for natural products with selectivity for an AChR subtype deserves special attention based on the perspective of developing drugs for novel therapeutic approaches.

The tree *Drimys winteri* (locally called Canelo), a member of the Winteraceae family and native of the Pacific side of Southern Chile, is characterized by large and glossy green leaves. Interestingly, the tree is considered sacred by the native people, Araucanians, due to its medicinal properties. The tree produces drimane sesquiterpenoids as secondary metabolites[6,7] including lactones with activity against bacterial quorum sensing[8] and the dialdehyde polygodial, which displays the strongest antifungal properties.[9]

To have a more comprehensive idea of the functional interaction of drimane sesquiterpenoids with different human (h) AChR subtypes, several compounds, including drimenin, cinnamolide, dendocarbin A, and polygodial (Figure 1), were purified from the bark extract of the *D. winteri* tree and chemically characterized by spectroscopic methods. The pharmacological activity of each compound was subsequently determined by Ca^{2+} influx-induced fluorescence detections using cell lines expressing hα4β2, hα3β4, or hα7 AChRs. Since the drimane sesquiterpenoids show relatively higher selectivity for the hα4β2 AChRs, correlations between the calculated inhibitory potencies and several physicochemical properties (i.e., polar surface area, lipophilicity, and molecular volume), hydrogen-bonding formation, molecular docking, and molecular dynamics were determined on the hα4β2 AChR model

Received: October 25, 2017
Published: April 10, 2018

DOI: 10.1021/acs.jnatprod.7b00893
J. Nat. Prod. 2018, 81, 811−817

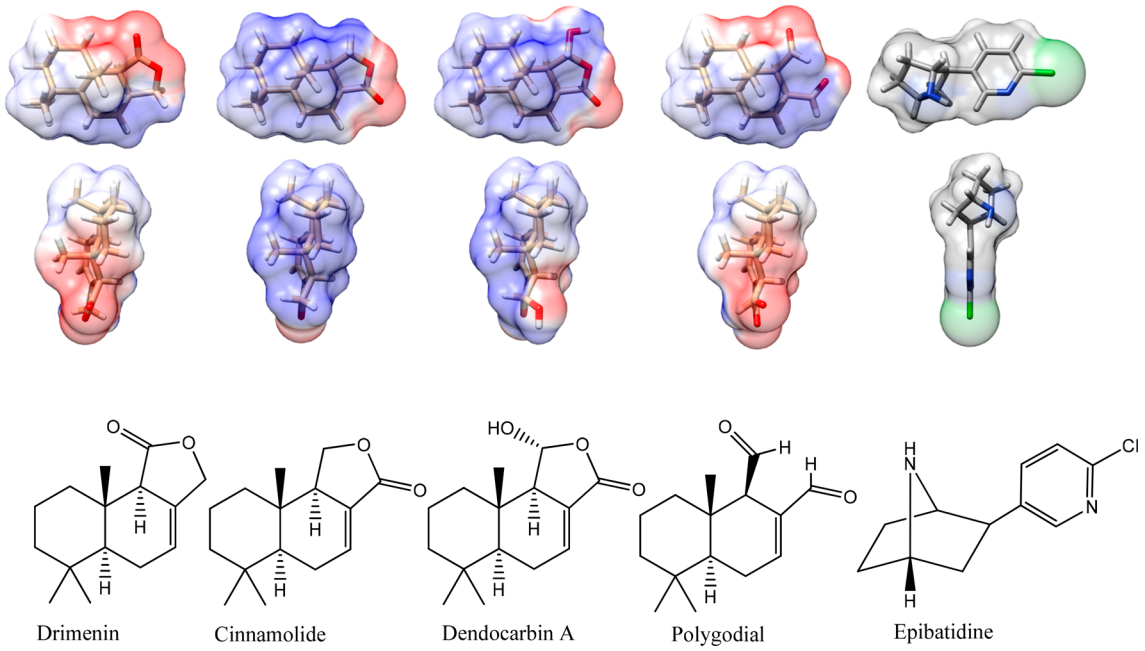

Figure 1. Molecular structures of drimane sesquiterpenoids purified from the barks of the Canelo tree, *D. winteri*, including drimenin [(5a*S*,9a*S*,9b*R*)-5a,6,7,8,9,9a-hexahydro-6,6,9a-trimethylnaphtho[2,1-*c*]furan-1(3*H*,5*H*,9b*H*)-one], cinnamolide [(5a*S*,9a*S*,9b*R*)-1,5a,6,7,8,9,9a,9b-octahydro-6,6,9a-trimethylnaphtho[2,1-*c*]furan-3(5*H*)-one], polygodial [(1*R*,4a*S*,8a*S*)-1,4,4a,5,6,7,8,8a-octahydro-5,5,8a-trimethylnaphthalene-1,2-dicarbaldehyde], and dendocarbin A [(1*R*,5a*S*,9a*S*,9b*R*)-1,5a,6,7,8,9,9a,9b-octahydro-1-hydroxy-6,6,9a-trimethylnaphtho[2,1-*c*]furan-3(5*H*)-one]. Each structure (as sticks, with oxygens in red) is surrounded by its molecular surface, where the electrostatic potential is colored from most negative (red) to most positive (blue). For comparative purposes, the structure of (−)-epibatidine with its characteristic chlorine group (green) is included.

using the recently determined X-ray crystal structure of the h$\alpha4\beta2$ AChR at 3.9 Å resolution.[10] In addition, two pharmacophore models for drimane sesquiterpenoids are described. The results show for the first time that drimane sesquiterpenoids, except dendocarbin A, inhibit AChR function in an allosteric fashion. Since these compounds show higher selectivity for h$\alpha4\beta2$ AChRs, drimenin could be used as a molecular scaffold for the development of more potent inhibitors with higher selectivity for $\alpha4\beta2$ AChRs.

RESULTS AND DISCUSSION

Chemical Characterization of Drimane Sesquiterpenoids. The drimane sesquiterpenoids drimenin, cinnamolide, dendocarbin A, and polygodial (Figure 1) were isolated from EtOAc extracts of the bark from the Canelo tree *D. winteri*. The ^{1}H NMR (Table S1, Supporting Information) and ^{13}C NMR (Table S2, Supporting Information) results are in excellent agreement with previous data.[11,12]

The chemical characterization of drimane sesquiterpenoids coincides with that obtained by X-ray studies,[13−15] where a basic structural framework is shown: a *trans*-decalin moiety with a $\Delta^{7(8)}$ double bond, giving a twisted chair conformation at the second ring and conferring a planar C-7−C-8−C-12 dihedral angle of 126.7° for dendocarbin A.

Pharmacologic Activity of Drimane Sesquiterpenoids on Different Human AChR Subtypes. The potency of (±)-epibatidine to activate each AChR subtype was first determined by assessing (±)-epibatidine-evoked fluorescence changes in cells expressing each particular AChR subtype, including the h$\alpha4\beta2$ (Figure 2A,B), h$\alpha3\beta4$ (Figure 3A), and h$\alpha7$ (Figure 3B). The observed EC_{50} values for (±)-epibatidine (29 ± 5 nM for h$\alpha4\beta2$; 12 ± 5 nM for h$\alpha3\beta4$, and 52 ± 4 nM for h$\alpha7$) are in the same concentration range as those reported.[16−19]

The agonistic activity of the drimane sesquiterpenoids (Figure 1) was subsequently tested by direct stimulation on each AChR subtype. In the case of h$\alpha4\beta2$ AChRs, the Ca^{2+} influx traces indicated that drimenin, opposite of (±)-epibatidine, does not have agonistic activity (Figure 2A). The same results were obtained for the other drimane sesquiterpenoids. The lack of agonistic activity was also observed on the h$\alpha3\beta4$ and h$\alpha7$ subtypes (not shown). On the other hand, the inhibitory activity of these natural compounds was assessed on each AChR subtype by preincubating each compound for 5 min before (±)-epibatidine stimulation. Figure 2A shows the traces of (±)-epibatidine in the presence of 1.0 μM drimenin, indicating that the compound inhibited agonist-evoked h$\alpha4\beta2$ AChR activity. All compounds, with the exception of dendocarbin A, produced the same inhibition but with different potency. In fact, whereas drimenin decreased (±)-epibatidine activity by 100% in the 10−100 μM concentration range, dendocarbin A was inactive at concentrations up to 100 μM. The observed inhibitory potency (IC_{50}) for the studied sesquiterpenoids at h$\alpha4\beta2$ AChRs follows the rank order drimenin ∼ cinnamolide > polygodial (Table 1). Similar results were obtained at the h$\alpha3\beta4$ (Figure 3A) and h$\alpha7$ (Figure 3B) subtypes, although polygodial was inactive in the h$\alpha7$ AChR. By comparing the IC_{50} values obtained at each AChR subtype, the following receptor selectivity was determined: h$\alpha4\beta2$ > h$\alpha3\beta4$ > h$\alpha7$. This is the first time that an inhibitory activity is shown by drimane sesquiterpenoids with relatively higher selectivity for h$\alpha4\beta2$ AChRs.

The calculated n_H values are in general higher than unity (Table 1), indicating that the observed inhibition is mediated by a cooperative mechanism. However, the n_H values for cinnamolide and polygodial at the h$\alpha4\beta2$ AChR and for

DOI: 10.1021/acs.jnatprod.7b00893
J. Nat. Prod. 2018, 81, 811−817

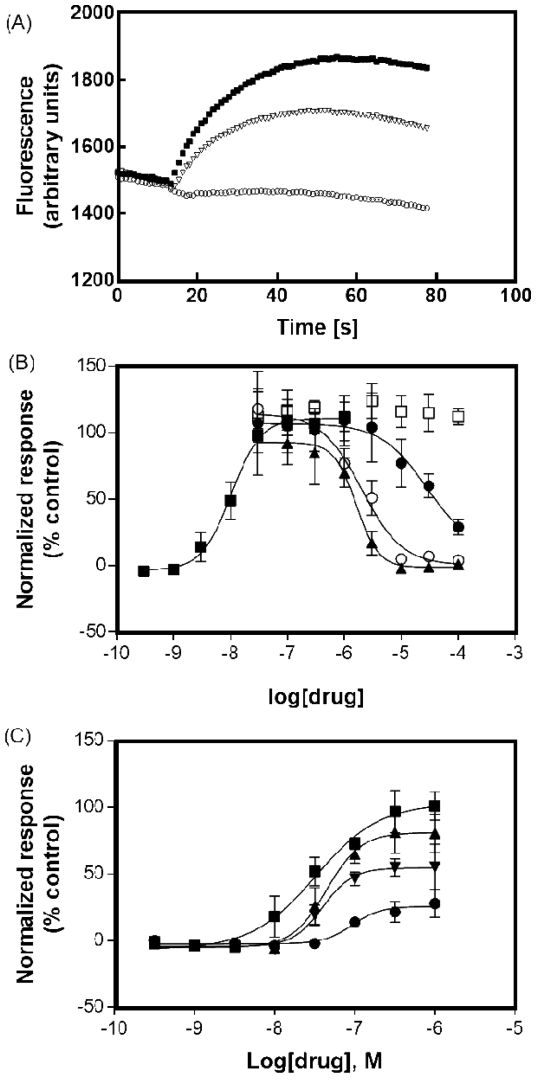

Figure 2. Functional activity of drimane sesquiterpenoids on HEK293-h$\alpha4\beta2$ cells by using Ca^{2+} influx measurements. (A) (±)-Epibatidine (1.0 μM) (■), but not drimenin (100 μM) (○), enhanced intracellular calcium. The same results were found for the other drimane sesquiterpenoids. Instead, 1.0 μM drimenin inhibited (±)-epibatidine-evoked h$\alpha4\beta2$ AChR activity (△). The same results were found for the other drimane sesquiterpenoids, except for dendocarbin A, which was inactive at concentrations up to 100 μM. (B) Increased concentrations of (±)-epibatidine (■) activated h$\alpha4\beta2$ with EC_{50} = 29 ± 5 nM (n = 24). The antagonistic activity of drimane sesquiterpenoids (n = 3) was investigated by pretreating (5 min) the cells with different concentrations of drimenin (▲), cinnamolide (○), polygodial (●), and dendocarbin A (□), respectively, followed by h$\alpha4\beta2$ activation with 0.1 μM (±)-epibatidine (■). The error bars represent the standard deviation (SD). Ligand response was normalized to the maximal (±)-epibatidine response, which was set as 100%. The calculated IC_{50} and n_H values are summarized in Table 3. (C) Concentration–activity response of (±)-epibatidine in the absence of drimenin (■) or after preincubation with 0.3 (▲), 1.0 (▼), and 3.0 (●) μM drimenin, respectively (n = 3). The results suggest a noncompetitive mechanism of inhibition.

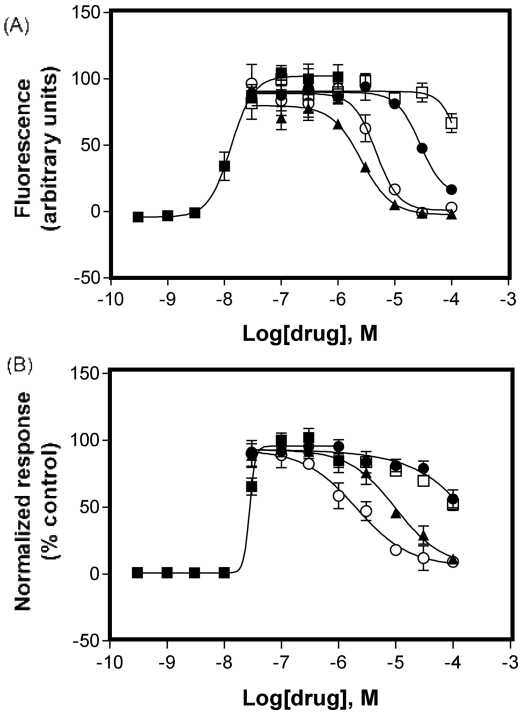

Figure 3. Functional activity of drimane sesquiterpenoids on HEK293-h$\alpha3\beta4$ (A) and GH3-h$\alpha7$ (B) cells by using Ca^{2+} influx measurements. The antagonistic activity of drimane sesquiterpenoids was investigated by pretreating (5 min) the cells with different concentrations of drimenin (▲), cinnamolide (○), polygodial (●), and dendocarbin A (□), respectively, followed by activation with 0.1 μM (±)-epibatidine (■). The error bars represent the standard deviation (SD) (n = 3). Ligand response was normalized to the maximal (±)-epibatidine response, which was set as 100%. The calculated IC_{50} and n_H values are summarized in Table 1.

Table 1. Inhibitory Potency (IC_{50}) of Drimane Sesquiterpenoids at Different Human AChRs

AChR subtype	drimane sesquiterpenoid	IC_{50} (μM)	n_H[c]
h$\alpha4\beta2$[a]	drimenin	0.97 ± 0.4	1.77 ± 0.37
	cinnamolide	1.57 ± 0.4	1.38 ± 0.32
	polygodial	62.5 ± 19.9	1.03 ± 0.24
	dendocarbin A	none	–
h$\alpha3\beta4$[b]	drimenin	1.78 ± 0.2	1.84 ± 0.16
	cinnamolide	2.62 ± 0.8	2.08 ± 0.10
	polygodial	48.2 ± 7.6	2.10 ± 0.87
	dendocarbin A	>100	–
h$\alpha7$[c]	drimenin	13.8 ± 6.6	1.68 ± 0.12
	cinnamolide	4.64 ± 2.4	1.03 ± 0.19
	polygodial	>100	–
	dendocarbin A	>100	–

[a]Values obtained from Figure 2B. [b]Values obtained from Figure 3A. [c]Values obtained from Figure 3B. [d]Hill coefficient.

cinnamolide at the h$\alpha7$ AChR, which are closer to unity (Table 1), suggest that the observed inhibition is mediated by a noncooperative mechanism.[20]

To determine the mechanism of inhibition elicited by drimane sesquiterpenoids on h$\alpha4\beta2$ AChRs, additional experiments were performed by determining the concentration–activity of (±)-epibatidine after preincubation with different concentrations of drimenin (Figure 2C). The results showing that the (±)-epibatidine maximal activity is decreased at higher drimenin concentrations are consistent with a noncompetitive mechanism of inhibition. Whether this mechanism is mediated by ion channel blocking or another allosteric mode of inhibition cannot be discriminated with this assay.

DOI: 10.1021/acs.jnatprod.7b00893
J. Nat. Prod. 2018, 81, 811–817

Table 2. Physichochemical Parameters for Drimane Sesquiterpenoids

parameter	drimenin	cinnamolide	polygodial	dendocarbin A	correlation coefficient[a] (*P* values)
polar surface area (PSA) (Å^2)	26.23	26.23	34.60	47.05	0.999 (0.005)
aqueous solubility (AS)	−4.67	−4.80	−4.03	−3.96	0.972 (0.106)
LogP (lipophilicity)	3.13	3.27	2.82	2.80	0.898 (0.207)
molecular volume (MV) (Å^3)	218.2	219.4	223.2	226.8	0.951 (0.142)

[a]The correlation coefficients between the calculated parameters and the determined IC_{50} values were obtained using the ligand IC_{50} values, excluding dendocarbin A, for the hα4β2 AChR (Table 1).

Correlation between the Pharmacological Activity of Drimane Sesquiterpenoids at hα4β2 AChRs and Their Physicochemical Parameters. To determine the structure−activity relationship for drimane sesquiterpenoids, a series of physicochemical parameters (i.e., PSA, AS, LogP, and MV) were first calculated (Table 2) and subsequently correlated with their IC_{50} values at hα4β2 AChRs (Table 1).

Although the correlations showed good r^2 values (0.898−0.972), the linear regressions showed no significant relationship (P = 0.106−0.142). Interestingly, a significant correlation was obtained for polar surface area (PSA) (r^2 = 0.999; P = 0.005) (Figure 4), indicating the following relationship: the lower the ligand polarity, the higher the affinity.

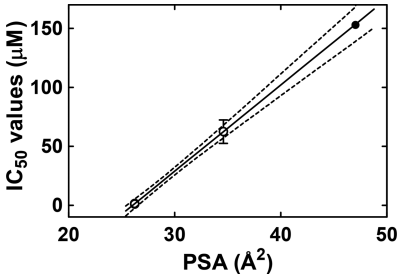

Figure 4. Correlation between the inhibitory potency (IC_{50}) of drimane sesquiterpenoids and their polar surface area (PSA) values. The IC_{50} values were taken from Table 1, whereas the PSA values were taken from Table 2. The linear regression obtained without the IC_{50} value for dendocarbin A showed an excellent correlation (r^2 = 0.999), with a slope significantly different from zero (P = 0.005). The 95% confidence intervals (---) are also included. A predicted IC_{50} value (>150 μM) for dendocarbin A (●) was subsequently calculated by plugging in its PSA value in the obtained linear regression.

Molecular Docking of Drimane Desquiterpenoids to the h(α4)$_3$(β2)$_2$ AChR. The DOPE score for the h(α4)$_3$(β2)$_2$ model was −257025, compared to −257162 for the X-ray hα4β2 AChR structure. A lower DOPE score (i.e., lower structural energy) indicates a better structural model.

Since the experimental results indicated a higher selectivity for h(α4)$_3$(β2)$_2$ AChRs, the docking experiments were performed using the same stoichiometry. Figure 5A shows the most important molecular interactions of drimenin with luminal and nonluminal (i.e., trans membrane domains (TMD) β2 intrasubunit site) sites. The average root-mean-square deviation (RMSD) and variance (VAR) values (i.e., < 1) obtained during the last third of the MD simulations indicated that these interactions are stable. The calculated binding affinity (CBA) values (calculated using the calculated binding energy (CBE) values) indicated that the ligands interact with the

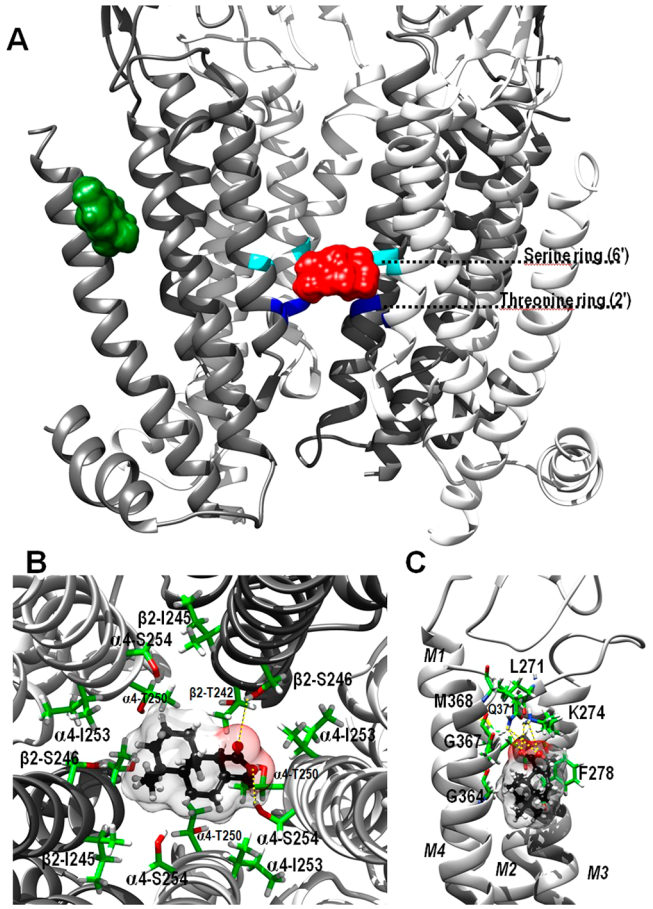

Figure 5. Docking sites for drimenin at the h(α4)$_3$(β2)$_2$ AChR model. (A) Stable docking sites for drimenin, including the luminal (red) and nonluminal intrasubunit β2 (green) sites. The α4 (white) and β2 (gray) subunits are represented as ribbons (one α4 subunit was omitted for clarity). Drimenin is represented as a molecular surface. (B) In the luminal site, drimenin interacted with M2 residues from both α4 and β2 subunits, forming H-bonds with both α4-S254 and β2-S246 (yellow lines). (C) In the intrasubunit β2 site, drimenin interacted only with β2-M3 and β2-M4 residues, forming two simultaneous H-bonds with β2-K274 and alternatively with β2-Q371 (yellow lines). The interacting residues (as sticks) (summarized in Table 4) are labeled by their subunit, residue one-letter code, and amino acid sequence number and colored by atoms, including carbons (green), nitrogens (blue), oxygens (red), sulfur (yellow), and hydrogen (white). Drimenin is represented as ball and sticks surrounded by their molecular surfaces and colored by atoms with carbons in black. Molecular images were generated using the UCSF Chimera package (supported by NIGMS P41-GM103311).

DOI: 10.1021/acs.jnatprod.7b00893
J. Nat. Prod. 2018, 81, 811−817

luminal site with slightly higher affinity compared to the values in the nonluminal site (Table 3), which in turn were closer to the rank of the experimental values.

Table 3. Luminal and Nonluminal Docking Sites for Drimane Sesquiterpenoids at the h(α4)$_3$(β2)$_2$ Model

site	domain	ligand	RMSD (VAR)[a]	CBE[b] (kcal/mol)
luminal	ion channel	drimenin	1.01 (0.025)	−196
		cinnamolide	0.80 (0.029)	−193
		polygodial	0.99 (0.006)	−196
nonluminal (intrasubunit β2)	TMD	drimenin	4.28 (0.042)	−182
		cinnamolide	4.17 (0.614)	−172
		polygodial	3.47 (0.412)	−147

[a]RMSD and variance (VAR) values were calculated during the last third of the MD simulations. [b]Calculated binding energy (CBE) values: the higher the negative value, the higher the calculated binding affinity (CBA).

The luminal site is situated approximately in the middle of the ion channel, from position 2′ (i.e., threonine ring) to 6′ (i.e., serine ring) (Figure 5A), comprising M2 residues α4-T250, α4-I253, α4-S254, β2-T242, β2-I245, and β2-S246 (Figure 5B; Table 4).

Table 4. Residues Involved in the Docking of Drimane Sesquiterpenoids to Luminal and Nonluminal Sites in the h(α4)$_3$(β2)$_2$ Model

		TMD	
site	ion channel M2 (position)	M3	M4
luminal	α4-T250 and β2-T242 (2′)		
	α4-I253 and β2-I245 (5′)		
	α4-S254 and β2-S246 (6′)		
nonluminal (intrasubunit β2)		β2-L271	β2-G364
		β2-K274	β2-G367
		β2-Y275	β2-M368
		β2-F278	β2-Q371

Drimenin formed two H-bonds, one between the α4-S254 hydroxy side chain and the ligand ring O and another between the β2-S246 hydroxy side chain and the ligand side chain O (Figure 5B). Similarly, polygodial formed two H-bonds, whereas cinnamolide formed one H-bond with α4-S254.

In the intrasubunit β2 site, the ligands interacted with exactly the same β2 residues from M3 (L271, K274, Y275, and F278) and M4 (G364, G367, M368, and Q371) (Figure 5C; Table 4). In particular, drimenin formed two simultaneous H-bonds with β2-K274, between two ligand oxygens and two amine hydrogens of the residue side chain (Figure 5C) and alternatively with β2-Q371.

The structure−activity relationship results at the hα4β2 AChR, indicating that the lower the ligand polarity, the higher the inhibitory potency, are in agreement with the proposed TMD location for the nonluminal site. In this scenario, the relatively lower polarity and higher lipophilic nature of drimenin and cinnamolide allowed them to diffuse within the receptor's TMD, reaching the β2 intrasubunit site, whereas ligands with relatively higher polarity and lower lipophilicity such as polygodial had difficulties reaching this site. The importance of this site at the hα4β2 AChR is consistent with the lower activity of these compounds at the hα3β4 and hα7 AChRs, which lack this particular site.

Pharmacophore for Drimane Sesquiterpenoids. Two alternative pharmacophore models were considered (Figure 6),

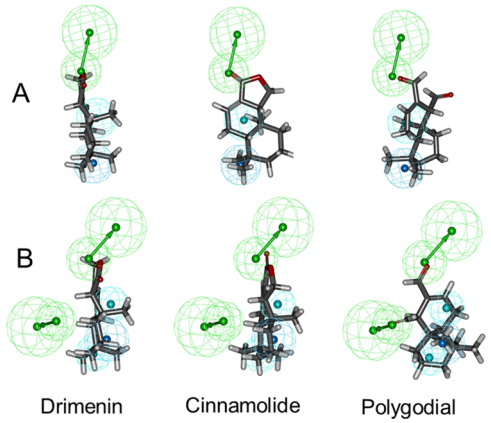

Figure 6. Pharmacophore models for drimane sesquiterpenoids based on either the experimental IC_{50} values (A) or the CBA values calculated for the intrasubunit β2 site located in the TMD of the h(α4)$_3$(β2)$_2$ model (B). Images show the geometrical and chemical features for each pharmacophore: Each point is represented as a small sphere. Hydrogen bond acceptor points are colored in green. Pure aliphatic hydrophobic centers are shown in cyan, or solely hydrophobic in light blue. Since H-bonds are directional, they are specified by two points, the location of the corresponding heavy atom of the ligand and the residue acceptor/donor, both connected by an arrow, which defines the direction of the H-bond. Each wired sphere defines the exclusion volume of a particular feature point (i.e., the maximum volume where the matching atoms can be positioned in the model).

one based on the experimental IC_{50} values for hα4β2 AChRs (Table 1) and the other based on the CBE values obtained for the β2 intrasubunit site (Table 3). Since the CBE values for the luminal site were similar for the three ligands, they could not be used to model the pharmacophore. The experimental-based pharmacophore consisted of one hydrogen bond acceptor point (HBAP, in green), two hydrophobic centers (HCPs), one pure aliphatic (in cyan), and another not entirely aliphatic (in light blue) represented as small spheres (Figure 6A).

The pharmacophore model for the β2 intrasubunit site showed a relatively better correlation (r^2 = 0.99), consisting of two HBAPs, three HCPs, two pure aliphatic, and another not entirely aliphatic (Figure 6B). Since H-bonds are directional, the HBAP feature is specified by two points connected by an arrow, the location of the corresponding heavy atom, and the other, which defines the direction of the H-bond. Each wired sphere defines the exclusion volume of a particular feature point (i.e., the maximum volume where the matching atoms can be positioned in the model due to steric hindrance).

In the β2 intrasubunit model, drimenin and cinnamolide aligned with only one H-bond, by means of the lactone oxygen in the first case and through the lactone carbonyl oxygen in the second case, whereas polygodial aligned with both H-bonds by means of the two oxygens of the carbonyl groups.

The pharmacophore models indicated that the activity of the ligands might be due to their capacity of forming H-bonds and making hydrophobic contacts with the receptor. These models are consistent with the proposed luminal and nonluminal sites,

DOI: 10.1021/acs.jnatprod.7b00893
J. Nat. Prod. 2018, 81, 811−817

where H-bonds and hydrophobic contacts (i.e., α4-I253 and β2-I245 in the luminal site; β2-L271, β2-Y275, β2-F278, and β2-M368 in the nonluminal site) were observed. Although the relative importance of the luminal vs nonluminal site in the overall inhibitory activity elicited by these compounds cannot be distinguished, the ligand interaction with both sites may inhibit the receptor by a cooperative mechanism. This is in agreement with the Ca^{2+} influx experiments, where n_H values higher than unity were calculated, suggesting the presence of more than one binding site and, thus, supporting additional allosteric modes of inhibition such as drug-induced receptor desensitization.[10]

This is the first time that a noncompetitive inhibitory activity of drimane sesquiterpenoids with relatively higher selectivity for hα4β2 AChRs is shown. Since hα4β2 AChRs are involved in the process of drug (and nicotine) addiction[5] and depressive states[21] and are also considered potential targets for structurally and functionally different antidepressants,[16−19,22] the observed inhibitory activity of drimane sesquiterpenoids could be exploited for the development of novel antiaddictive and antidepressant ligands. In fact, the calculated potency for drimenin at the hα4β2 AChR (0.97 ± 0.35 μM) is several fold higher than that for other clinically used antidepressants using the same method, including bupropion (17.8 ± 2.2 μM),[19] (−)-reboxetine (16.0 ± 1.0 μM),[18] imipramine (5.4 ± 1.2 μM),[17] and fluoxetine (4.4 ± 0.6 μM).[16] In this regard, drimenin could be used as a molecular scaffold for the development of more potent noncompetitive antagonists with higher selectivity for the hα4β2 AChR.

EXPERIMENTAL SECTION

Materials. (±)-Epibatidine hydrochloride was obtained from Tocris Bioscience (Ellisville, MO, USA). Fetal bovine serum (FBS) and trypsin/EDTA were purchased from Gibco BRL (Paisley, UK). Ham's F-12 nutrient mixture was obtained from Invitrogen (Paisley, UK). Solvents used in this study were distilled prior to use and dried over appropriate drying agents. Salts were of analytical grade.

Purification of Drimane Sesquiterpenoids from *Drimys winteri*. Barks of *D. winteri* were collected in Temuco, IX Region of Chile, in February 2015. Bark (4.5 kg) was initially crushed and extracted by maceration with EtOAc (6 L) for 3 d. The organic layer was evaporated *in vacuo*, giving a crude product (60 g), which was further purified by column chromatography, giving a primary fractioning of eight fractions (F1−F8) by using increasing polarity from hexane to EtOAc. A subsequent chromatographic purification of F3 with *n*-hexane/EtOAc (9:1 v/v) gave drimenin (600 mg, colorless crystals, 0.013% yield) followed by cinnamolide (320 mg, colorless crystals, 0.0071% yield), whereas the purification of F4 with *n*-hexane/EtOAc (8:2 v/v) gave polygodial (950 mg, yellow oil, 0.021% yield), and the purification of F6 with *n*-hexane/EtOAc (1:1 v/v) gave dendocarbin A (60 mg, colorless crystals, 0.0013% yield). The compounds were confirmed by TLC using pure standards previously characterized by spectroscopic methods.

Chemical Analysis of Drimane Sesquiterpenoids. Optical rotations were recorded on a JASCO P-200 polarimeter (Tokyo, Japan). FTIR spectra were measured on a Nicolet 6700 from Thermo Electron Corporation with the ATR-unit Smart Performer. Melting points were determined on a Melting Point SMP10 (Stuart) and are uncorrected. The ^1H and ^{13}C NMR spectra were recorded in CD_2Cl_2 or $CDCl_3$ solution in 5 mm tubes at room temperature on a Bruker Avance III spectrometer (Bruker Biospin GmbH, Rheinstetten, Germany) at 600.13 (^1H) and 150.61 (^{13}C) MHz, with the deuterium signal of the solvent as the lock and tetramethylsilane (for ^1H) or the solvent (for ^{13}C) as internal standard. All spectra (^1H, ^{13}C, gs-H,H−COSY, edited HSQC, and gs-HMBC) were acquired and processed with the standard Bruker software. The ^1H and ^{13}C NMR results are summarized in Tables S1 and S2 (Supporting Information), respectively.

Ca^{2+} Influx Measurements in HEK293-hα4β2, HEK293-hα3β4, and GH3-hα7 Cells. Ca^{2+} influx measurements were performed on HEK293-hα4β2, HEK293-hα3β4, and GH3-hα7 cells as previously described.[16−19] Briefly, 5×10^4 cells per well were seeded 72 h prior to the experiment on black 96-well plates (Costar, New York, USA) and incubated at 37 °C in a humidified atmosphere (5% CO_2/95% air). Under these conditions, the majority of expressed hα4β2 and hα3β4 AChRs have the $(\alpha x)_3(\beta x)_2$ stoichiometry.[19] Sixteen to 24 h before the experiment, the medium was changed to 1% FBS in HEPES-buffered salt solution (HBSS) (130 mM NaCl, 5.4 mM KCl, 2 mM $CaCl_2$, 0.8 mM $MgSO_4$, 0.9 mM NaH_2PO_4, 25 mM glucose, 20 mM HEPES, pH 7.4). On the day of the experiment, the medium was removed by flicking the plates and replaced with 100 μL HBSS/1% FBS containing 2 mM Fluo-4 (Molecular Probes, Eugene, OR, USA) in the presence of 2.5 mM probenecid (Sigma, Buchs, Switzerland). The cells were incubated at 37 °C in a humidified atmosphere (5% CO_2/95% air) for 1 h.

To determine the antagonistic activity of the drimane sesquiterpenoids, plates were flicked to remove excess Fluo-4, washed twice with HBSS/1% FBS, refilled with 100 μL of HBSS containing the ligand under study, and incubated for 5 min. Plates were finally placed in the cell plate stage of the fluorimetric imaging plate reader (FLIPR; Molecular Devices, Sunnyvale, CA, USA), and (±)-epibatidine (0.1 μM) was added from the agonist plate to the cell plate using the 96-tip pipettor simultaneously to fluorescence recordings for a total length of 78 s. A baseline consisting of five measurements of 0.4 s each was previously recorded. To determine the agonistic activity of the drimane sesquiterpenoids or (±)-epibatidine, each compound was added to the cell plate and the fluorescence recorded for 78 s. In parallel experiments, the concentration−activity response of (±)-epibatidine was determined in the absence of drimenin or after 5 min of preincubation with different concentrations of drimenin (i.e., 0.3, 1.0, and 3.0 μM). The excitation and emission wavelengths are 488 and 510 nm, at 1 W with a CCD camera opening of 0.4 s. The concentration−response data were curve-fitted by nonlinear least-squares analysis using the Prism software (GraphPad Software, San Diego, CA, USA).

Calculated Determination of the Physicochemical Properties of Drimane Sesquiterpenoids. To determine the physicochemical properties of drimane sesquiterpenoids, several parameters were calculated using Accelrys Discovery Studio 2.5. These parameters include lipophilicity (LogP), polar surface area (PSA) [i.e., surface area (Å^2) occupied by nitrogen and oxygen atoms and the polar hydrogens attached to them], aqueous solubility (AS), and molecular volume (MV, Å^3).

Homology Model of the h$(\alpha4)_3(\beta2)_2$ AChR Using the hα4β2 Crystal Structure. Since drimane sesquiterpenoids showed higher selectivity for the hα4β2 AChR (Table 1), the subsequent molecular modeling studies were performed using the h$(\alpha4)_3(\beta2)_2$ AChR model. The h$(\alpha4)_3(\beta2)_2$ AChR model was built using the X-ray structure (PDB ID: 5KXI) of the hα4β2 AChR at 3.9 Å resolution.[10] The h$(\alpha4)_3(\beta2)_2$ stoichiometry was modeled and evaluated following previous procedures.[19] The template X-ray h$(\alpha4)_2(\beta2)_3$ structure has two contiguous β2 subunits (between the "+" side of one of the two α4 subunits and the "−" side of the other α4), one of which was replaced by an α4 subunit to get the h$(\alpha4)_3(\beta2)_2$ stoichiometry. Arbitrarily the β2 subunit at the "+" side of one of the α4 subunits was replaced by a copy of this same α4. To place the new α4 subunit in the pentamer, its backbone atoms were aligned to those of the replaced β2. Subsequently, the model was energy minimized using molecular mechanics and the software NAMD and the CHARMM force field. During a first minimization, no Morse functions and no cross terms were used and the steepest descents method was employed. To avoid distorting the protein secondary structure, this energy minimization was carried out fixing the backbone atoms to their original positions. The structure was minimized until the maximum derivative was less than 2.00 kcal Å^{-1}. In a second step, the model was further minimized until the maximum derivative was less than 0.05 kcal Å^{-1}, with the

DOI: 10.1021/acs.jnatprod.7b00893
J. Nat. Prod. 2018, 81, 811−817

same constraints for the backbone atoms, but using the full model, with Morse functions and cross terms, and employing the conjugate gradients method.

Molecular Docking and Molecular Dynamics. Each compound was modeled and minimized, and its partial charge calculated using the MOPAC program as previously described.[19] Each molecule was subsequently docked into the $h(\alpha4)_3(\beta2)_2$ model using AutoDock Vina. The whole receptor model was used as a target. The parameters used were as follows: exhaustiveness = 570 (the maximum value allowed by our computational system) and maximum number of modes = 20. To achieve dockings in a few minutes' time regime, no flexible residues were allowed in the receptor model. The program gives clusters of superposed conformations from the 20 lowest energy binding poses.

To determine the stability of each of the 20 poses within its predicted docking site, 20 ns molecular dynamics (MD) simulations were performed as previously described.[17] The $h(\alpha4)_3(\beta2)_2$ AChR was first hydrated with a 10 Å minimum thick shell using the program Solvate 1.0, which also added the appropriate number of Cl^- and Na^+ to neutralize the system. Subsequently, the model was minimized using NAMD. The MD protocol includes a time step size of 1 fs, with 20 time steps per cycle (the number of time steps between atom reassignments). The cutoff value for nonbond energy evaluation was 12 Å. A distance of 8 Å for the switching function was used. Pairs of bonded atoms excluded from nonbonded interaction calculations were determined as 1−4; that is, no nonbonded interactions were calculated for lists of four consecutive bonded atoms.

The RMSD with respect to the initial structure was calculated.[19] The poses with VAR RMSD values of <1 during the last third of the MD were considered stable.

Calculation of the Calculated Binding Energies. Calculated binding energies, measured from the individual poses at the end of every MD, were calculated using molecular mechanics as follows:[23]

$$\mathrm{TBE} = C_{\mathrm{ENERGY}} + L_{\mathrm{ENTROPY}} - (L_{\mathrm{ENERGY}} + R_{\mathrm{ENERGY}}) \quad (1)$$

where *C* is the complex between the ligand (L) and the receptor (R). The CBE values are estimations used only for comparative purposes among ligands and do not intend to represent absolute binding energies. More negative CBE values indicate higher CBAs.

Pharmacophore Calculations. To complement the molecular docking studies, the 3D pharmacophore for drimane sesquiterpenoids was calculated using Accelrys Discovery Studio 2.5. A pharmacophore[24] is a group of steric and electronic characteristics and their corresponding 3D locations that are estimated to be essential and responsible for similar pharmacological activities. In this regard, the pharmacophore was calculated by using the experimental IC_{50} values as well as the CBE values of the intrasubunit $\beta2$ site. We considered this as the best binding site to use for this purpose for two reasons: (1) the high inverse correlation between inhibitory potency and drug surface polarity (Figure 4) indicates that a polar environment, as the one existing within the ion channel, is less likely to represent the main site of action of drimane sesquiterpenoids; (2) not only is the intrasubunit $\beta2$ site accessible through a nonpolar environment, but the calculated affinity estimations of drimane sesquiterpenoids follow the rank order of the experimental inhibitory potencies.

■ ASSOCIATED CONTENT

Supporting Information

The Supporting Information is available free of charge on the ACS Publications website at DOI: 10.1021/acs.jnatprod.7b00893.

Figure of molecular dynamics simulations of drimane sesquiterpenoids interacting with luminal and non-luminal sites in the $(\alpha4)_3(\beta2)2$ model; tables of ^1H and ^{13}C NMR data for drimane sesquiterpenoids purified from *D. winteri* (PDF)

■ AUTHOR INFORMATION

Corresponding Author

*Tel/Fax: +56-45-2325424. E-mail: cristian.paz@ufrontera.cl.

ORCID

Cristian Paz: 0000-0002-4668-4984

Notes

The authors declare no competing financial interest.

■ ACKNOWLEDGMENTS

This study was supported by grants from the Universidad de La Frontera (DI17-0049), REDI170107 from CONICYT (to C.P.), and California Northstate University College of Medicine (to H.R.A.).

■ REFERENCES

(1) Ortells, M. O. *Neurotransmitter* **2016**, *3*, e1273.
(2) Posadas, I.; López-Hernández, B.; Ceña, V. *Curr. Neuropharmacol.* **2013**, *11* (3).
(3) Dineley, K. T.; Pandya, A. A.; Yakel, J. L. *Trends Pharmacol. Sci.* **2015**, *36*, 9610.1016/j.tips.2014.12.002.
(4) Fuenzalida, M.; Pérez, M. Á.; Arias, H. R. *Curr. Pharm. Des.* **2016**, *22* (14), 2004−2014.
(5) Ortells, M. O.; Arias, H. R. *Int. J. Biochem. Cell Biol.* **2010**, *42* (12), 1931−1935.
(6) Appel, H. H.; Bond, R. P. M.; Overton, K. H. *Tetrahedron* **1963**, *19* (4), 635−641.
(7) Asakawa, Y.; Agnieszak, A.; Harinantenaina, L.; Toyota, M.; Nishiki, M.; Bardon, A.; Nii, K. *Nat. Prod. Commun.* **2012**, *7*, 685−692.
(8) Carcamo, G.; Silva, M.; Becerra, J.; Urrutia, H.; Sossa, K.; Paz, C. *J. Chil. Chem. Soc.* **2014**, *59*, 2622−2624.
(9) Kubo, I.; Lee, S. H.; Shimizu, K. *Open J. Med. Microbiol.* **2011**, *19*, 1013−1017.
(10) Morales-Perez, C. L.; Noviello, C. M.; Hibbs, R. E. *Nature* **2016**, *538* (7625), 41110.1038/nature19785.
(11) Rukachaisirikul, V.; Khamthong, N.; Sukpondma, Y.; Phongpaichit, S.; Hutadilok-Towatana, N.; Graidist, P.; Sakayaroj, J.; Kirtikara, K. *Arch. Pharmacal Res.* **2010**, *33*, 375−380.
(12) Rodríguez, B.; Zapata, N.; Medina, P.; Viñuela, E. *Magn. Reson. Chem.* **2005**, *43* (1), 82−84.
(13) Brito, I.; López-Rodríguez, M.; Zárraga, M.; Paz, C.; Pérez, C. *Acta Crystallogr., Sect. E: Struct. Rep. Online* **2008**, *64*, o738−o738.
(14) Brito, I.; López-Rodríguez, M.; Zárraga, M.; Paz, C.; Pérez, C. *J. Chil. Chem. Soc.* **2008**, *59*, 1732−1733.
(15) Paz, C.; Burgos, V.; Suarez, S.; Baggio, R. *Acta Crystallogr., Sect. C: Struct. Chem.* **2015**, *71*, 294−297.
(16) Arias, H. R.; Feuerbach, D.; Targowska-Duda, K. M.; Russell, M.; Jozwiak, K. *Biochemistry* **2010**, *49*, 5734−5742.
(17) Arias, H. R.; Rosenberg, A.; Targowska-Duda, K. M.; Feuerbach, D.; Jozwiak, K.; Moaddel, R.; Wainer, I. W. *Int. J. Biochem. Cell Biol.* **2010**, *42*, 1007−1018.
(18) Arias, H. R.; Fedorov, N. B. B.; Benson, L. C. C.; Lippiello, P. M. M.; Gatto, G. J. J.; Feuerbach, D.; Ortells, M. O. *J. Pharmacol. Exp. Ther.* **2013**, *344*, 113−123.
(19) Arias, H. R.; Feuerbach, D.; Ortells, M. O. *Neurochem. Int.* **2016**, *100*, 67−77.
(20) Gumilar, F.; Arias, H. R.; Spitzmaul, G.; Bouzat, C. *Neuropharmacology* **2003**, *45*, 964−976.
(21) Mineur, Y. S.; Picciotto, M. R. *Trends Pharmacol. Sci.* **2010**, *31*, 580−586.
(22) García-Colunga, J.; Targowska-Duda, K. M.; Arias, H. R. *Neurotransmitter* **2016**, *3*, 1293.
(23) Tirado-Rives, J.; Jorgensen, W. L. *J. Med. Chem.* **2006**, *49*, 5880−5884.
(24) Li, H.; Sutter, J.; Hoffmann, R. In *Pharmacophore Perception, Development, and Use in Drug Design*; Güner, O. F., Ed.; International University Line: La Jolla, CA, USA, 2000; pp 173−189.

DOI: 10.1021/acs.jnatprod.7b00893
J. Nat. Prod. 2018, 81, 811−817